DOE GRANT # DE FG 02-05ER84298

A VERY HIGH SPATIAL RESOLUTION DETECTOR FOR SMALL ANIMAL PET

FINAL REPORT

March 6, 2007

Kanai Shah, PI

E. PHASE I FINAL REPORT

1. OVERVIEW

The main goal of the Phase I research was to demonstrate the feasibility of producing high resolution CdTe/CZT detectors for small animal PET imaging. The primary focus of the Phase I research was on investigation of the orthogonal strip detector design shown in **Figure 1**, although multi-pixel detector designs were also evaluated. In order to achieve the overall Phase I goal, the Phase I research covered several diverse areas. Simulation studies were conducted to analyze the timing characteristics of the proposed CdTe/CZT strip detectors. CdTe/CZT detectors were fabricated with orthogonal strip as well as multi-pixel designs and these detectors were packaged. Electronic read-out issues were addressed. Energy and timing resolution as well as spatial response were measured using 511 keV gamma-rays. Based on the results, the feasibility of the proposed effort was adequately demonstrated. The Phase I effort was a collaboration between RMD and Dr. Simon Cherry's group at UC-Davis. Dr. Zhong He at the University of Michigan (Ann Arbor) also participated in the Phase I effort and contributed towards the simulation studies.

2. SIMULATION STUDIES OF CdTe/CZT STRIP DETECTORS

The focus of the proposed effort is to develop high performance double-sided CdTe/CZT strip detectors for small animal PET imaging. One of the primary considerations in use of CdTe/CZT for PET imaging is the timing resolution that can be achieved with such detectors. In order to analyze timing characteristics of CdTe/CZT detectors for PET (with design shown in **Figure 1**) simulation studies were conducted in the Phase I effort in collaboration with Dr. Zhong He's group at the University of Michigan (Ann Arbor). We used Monte Carlo based methods to analyze the detector performance, particularly its temporal response. In order to evaluate the performance of double sided CdTe/CZT detectors for PET applications, the induced signal in the readout circuitry needed to be modeled as a function of time and spatial location. For this, the following steps are required:

Step 1: Model the internal electric field and the weighting potential as a function of electrode configurations and applied bias. This involves two tasks. First, we model the weighting potential function for given electrode configuration. It provides an effective "detector response function" that quantifies induced signals resultant from the movement of a unit space charge present at certain temporal and spatial location [Ramo]. Secondly, we model the actual internal electric field to determine the trajectory of charge carriers in the detector. This modeling was performed using the electromagnetic transport package, *Maxwell*, available in Dr. Zhong He's laboratory at the University of Michigan.

Step 2: Model typical gamma ray interactions in CdTe/CZT using a particle transport code, *GEANT4*, that is also available in Dr. He's laboratory at the University of Michigan.

Using these packages, Dr. He's team carried out simulations of timing characteristics as well as efficiency of the orthogonal strip CdTe/CZT detector with design shown in **Figure 1**. As shown in **Figure 1**, the detector consists of a 20x20 mm^2 CdTe/CZT slab with 0.5 mm thickness. On one 20x20 mm^2 slab, high resolution strips with 0.5 mm pitch are placed, while on the opposite face, wider strips with 2.5 mm pitch are placed (orthogonal to the 0.5 mm strips). The detector is

designed for irradiation on the edge (0.5x20 mm^2 face). The 2.5 mm strips are designed for operation as cathode strips and provide depth-of-interaction, while the 0.5 mm strips are operated as anode strips. These anode strips, in combination with detector thickness of 0.5 mm, provide localization of a 511 keV event within an effective pixel size of 0.5x0.5 mm^2.

Estimation of timing response for this detector design was carried out by considering the effect of electronic noise and the variation of (pre-amplifier) signal pulse waveforms. By using the electrostatic simulation program - *Maxwell*, the weighting potential of strip anodes was calculated as a function of detector depth and the result is shown in **Figure 8**. As seen in the figure, the weighting potential of an individual anode strip is very close to a straight line, showing that an anode strip electrode having a width of 0.4 mm (pitch of 0.5 mm) can be treated as a conventional planar electrode. This is because their width of 0.4 mm is comparable to the detector thickness of 0.5 mm. The weighting potential of a strip electrode could differ significantly from that of a planar electrode (a straight line) only if its width is much smaller than the thickness.

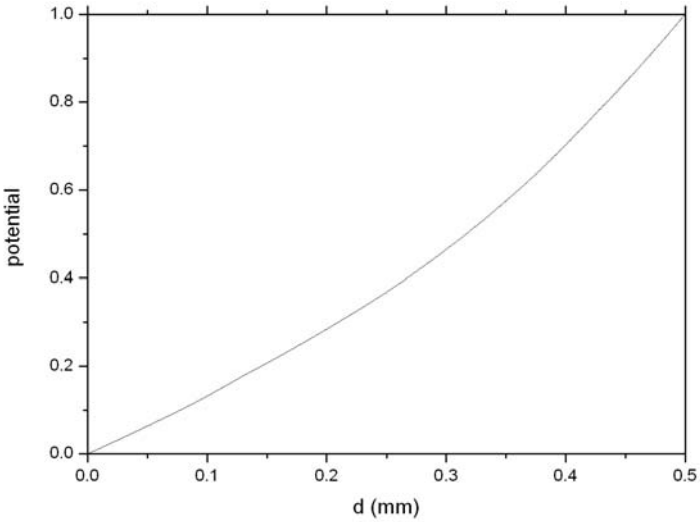

Figure 8. Simulated weighting potential as a function of detector depth (d) for a high resolution strip (0.4 mm width, 0.5 mm pitch) of the proposed detector shown in **Figure 1**.

In order to predict the preamplifier output signals for the anode strips, the detector bias (applied to cathode with negative polarity) was assumed to be 200 V. Using the published mobilities of electrons and holes in CdTe/CZT of 1000 $cm^2/V{\cdot}s$ and 65 $cm^2/V{\cdot}s$ respectively [Knoll], the drift velocities were determined to be 0.04 mm/ns and 0.0026 mm/ns for electrons and holes, respectively. The output signal pulse waveforms can be simulated by coupling together the charge drift process and the charge induction process. The simulated results are shown in **Figure 9**. Different pulse waveforms (shown in different colors) correspond to events of different interaction depth between the cathode and the anode surfaces. The anode surface was set to be 0 mm and the cathode surface was 0.5 mm. Assuming that the electronic noise is about 2% of the 511 keV photo-peak amplitude, the low-energy threshold for leading-edge timing trigger could be set at

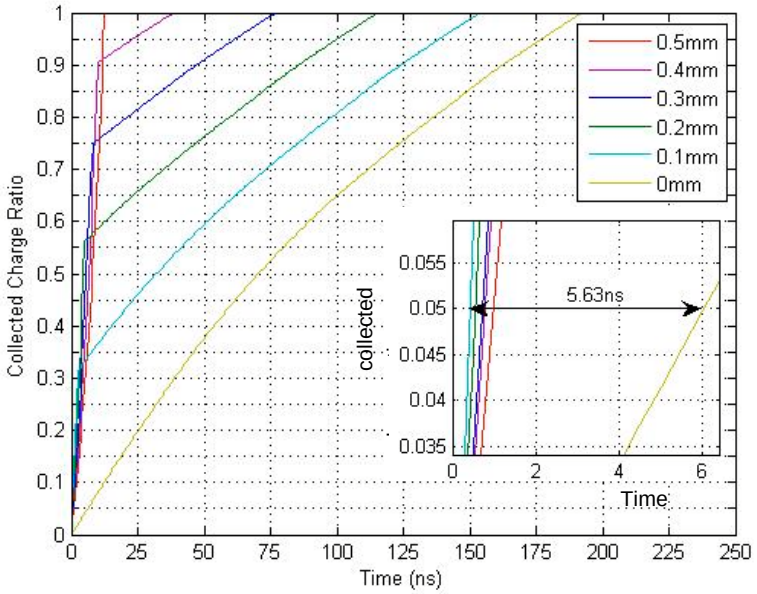

Figure 9. Simulated pulse waveforms for events occurring at different depths (distance from the anode plane) within the detector. The inset shows expanded view near the origin.

about 5% of the photo-peak amplitude in the waveform plot (the triggering threshold is about 2 times the electronic noise). The maximum timing variation (without noise) can be estimated to be about 5.6 ns as shown in the inset in **Figure 9**. If we include the electronic noise on pulse waveforms (see illustration in **Figure 10**), the maximum timing variation should be ~6.6 ns, which would represent the upper limit of timing resolution in absence of other effects. The timing resolution would be expected to improve as the detector bias is increased, which was indeed observed in our experiments.

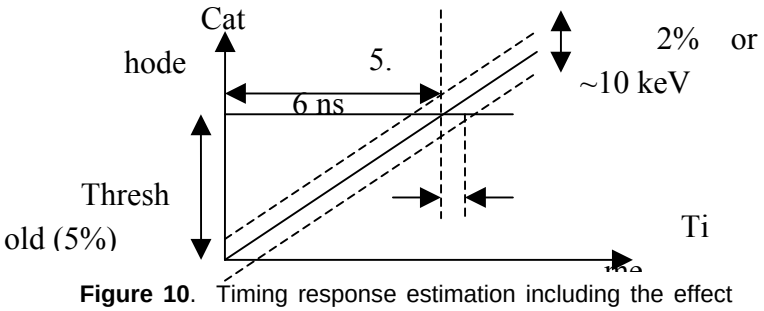

Figure 10. Timing response estimation including the effect of electronic noise on pulse waveform

Overall, this timing analysis using detector simulations is very encouraging because it indicated that high timing resolution can indeed be achieved with the proposed design of CdTe/CZT detectors.

Detector efficiency estimations were also carried out using *GEANT4* for 511 keV interaction in one CdTe/CZT detector orthogonal strip detector slice for irradiation on the edge as shown in **Figure 1**. The total efficiency for 511 keV γ-rays in single detector was estimated to be 62.1%, with Compton interaction contribution being 51.1% and Photoelectric interaction contribution of 11%. These efficiency numbers are for single 511 keV events (i.e not for coincidence events). As discussed earlier, both photoelectric and single interaction Compton events will be considered "good" events in the proposed detection scheme in order to achieve high detection efficiency.

One concern when stacking multiple "thin" detectors together in very high resolution applications, as proposed here, is the effect of inter-detector scatter. Simulations by Dr. Cherry's group [Stickel and Cherry] indicated very little degradation in the modulation transfer function for stacked CdTe detectors compared with single detectors, assuming that each strip detector is read out individually. Thus the stacking of detectors into modules to provide better solid angle coverage improves sensitivity without significantly compromising spatial resolution.

3. Fabrication and Packaging of CdTe/CZT Orthogonal Strip and Multi-Pixel Detectors

During the Phase I project, we investigated prototype CdTe/CZT arrays for PET imaging of small animals. The detectors were designed to provide high spatial resolution, high energy resolution, high timing resolution and high sensitivity for 511 keV gamma-rays used in PET imaging. The primary focus in the Phase I effort was on the fabrication and evaluation of orthogonal strip detectors with design shown in **Figures 1 and 11**.

The orthogonal strip CdTe/CZT detector is

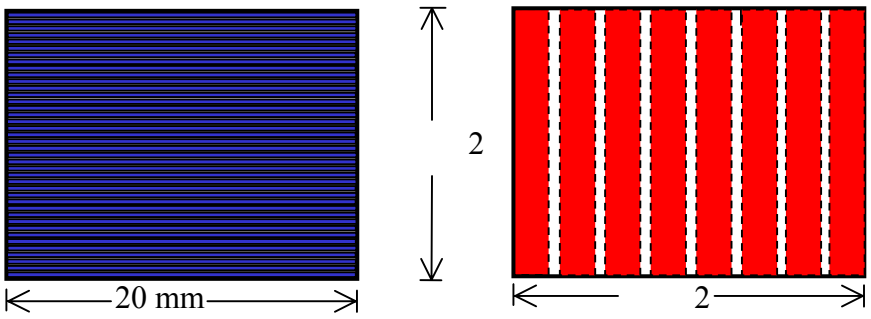

Figure 11. Two dimensional views of two 20x20 mm^2 faces of the proposed double sided CdTe/CZT strip detector with 0.5 mm thickness. On left the high resolution strips (~0.5 mm pitch) are shown in blue. On right, coarser strips (2.5 mm pitch) placed orthogonally to the high resolution strips are shown in red. Both sets of strips were fabricated using photolithography.

designed with 20x20 mm^2 area and 0.5 mm depth. On one 20x20 mm^2 face, fine strips with 0.5 mm pitch are placed, while on the other 20x20 mm^2 face, coarser strips with 2.5 mm pitch are placed orthogonally to the finer strips. The detector is designed for irradiation on the edge (i.e the 0.5x20 mm^2 face) as shown in **Figure 1**. Thus, 20 mm depth of CdTe/CZT is available to stop the 511 keV gamma-rays in order to achieve high detection efficiency. The spacing between anode and cathode faces is kept to 0.5 mm in order to provide fast and efficient collection of electron-hole pairs. As a result, high energy and timing resolution can be expected. The thickness of 0.5 mm along with fine strips with a pitch of 0.5 mm create an effective pixel size of 0.5x0.5 mm^2 for incoming gamma-rays, and as a result, excellent spatial resolution can be expected. Finally, the coarser strips with 2.5 mm pitch should provide very high depth-of-interaction (DOI) resolution.

In addition to orthogonal strip detectors, we also fabricated and evaluated small, multi-pixel CdTe/CZT arrays in the Phase I effort. These detectors were designed with 0.6 mm pixels in a 6x6 element format with 1 mm thickness. Eventually, stacks of such detectors can be arranged to achieve high efficiency and spatial resolution as well as high energy and timing resolution. Furthermore, due to this stacking configuration, high DOI resolution can also be expected. The main advantage of the orthogonal strip configuration over the multi-pixel array design is the reduction in the number of electronic channels (for strip design) for similar detector volume and anode-to-cathode spacing per element.

To build these detector configurations, CdTe and CZT crystals (with up to 20x20 mm^2 area and ~0.5-1 mm thickness) were purchased from commercial vendors such as Acrorad (in Japan) and Yinnel Tech. (South Bend, IN), respectively. These crystals were lapped and polished using alumina grits with appropriate particle sizes. The crystals were etched using 5% bromine in methanol solution. Gold electrodes that form ohmic contacts on CdTe/CZT crystals were used to create the orthogonal strips as well as multi-pixel arrays. For fabrication of orthogonal strip detectors, we used CdTe crystals and detectors supplied by Acrorad and the appropriate anode and cathode strips were deposited using photolithography. Photographs of both faces of such a strip detector were shown earlier in **Figure 2**. For creating multi-pixel CdTe and CZT arrays, gold electrodes were deposited using thermal evaporation process through appropriate shadow masks. The cathode face for multi-pixel arrays was continuous while the anode face was patterned to create 6x6 elements (0.6 mm pixels, 1 mm thickness). **Figure 12** shows a photograph of a CdTe multi-pixel array fabricated in this manner, which was then passivated. Similar CZT arrays were also fabricated in the Phase I effort. Surface passivation has been found to decrease surface leakage currents in CdTe/CZT devices and improve detector stability [Wright]. Surface passivation may be accomplished by various techniques involving chemical and

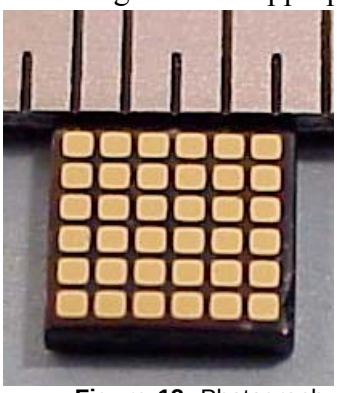

Figure 12. Photograph of CdTe multi-pixel array (0.6 mm pixels, 1 mm spacing) built in Phase I effort.

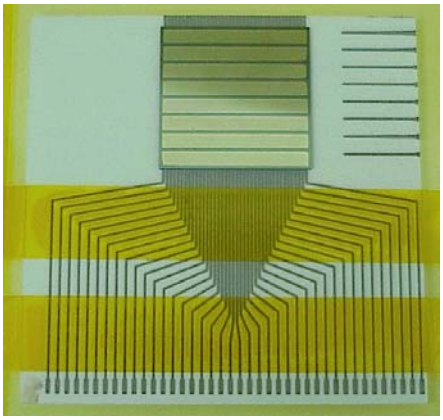

Figure 13. Photograph of packaged CdTe orthogonal strip detector. The coarser strips are seen on the top, while the fan-out traces at bottom provide connection to the finer strips.

physical processes. We followed a wet chemical oxidation process. Contacted devices were immersed in an aqueous solution of NH_4F in H_2O_2 [Wright] followed by drying in air. CdTe and CZT detectors were then packaged.

As shown in **Figure 13** (for an orthogonal strip CdTe detector), ceramic substrates with matching electrode patterns as well as fan-out to read all elements were designed, and the CdTe/CZT detectors were mated to such substrates using polymer-based bump bonding process developed by Polymer Assembly Technology (Billerica, MA). This technology utilizes conductive polymer bumps (consisting of silver filled conductive epoxy) to connect the pixels to a matching pattern on a substrate or an ASIC. The polymer bumps are screen-printed and can be sized to ≤50 μm. A primary advantage of this technology is the low processing temperature (about 65 °C) which greatly reduces the possibility of CdTe/CZT being degraded during the packaging procedure. A non-conductive polymer is filled in the vacant space between the substrate and the CdTe/CZT detectors and the polymers are cured. **Figure 13** shows a photograph of the packaged orthogonal strip detector with the coarser strips facing up. The fan-out arrangement seen at the bottom of the picture depicts the traces that are connected to the finer strips located on the back-side of the detector. For the coarser strips on the top, wires were connected from each strip to the parallel traces shown on the substrate on the right. Electrical connections were made from the ceramic substrate to the discrete readout electronics or the available ASICs to evaluate the detector. Similar arrangement was used for packaging of the multi-pixel CdTe/CZT arrays.

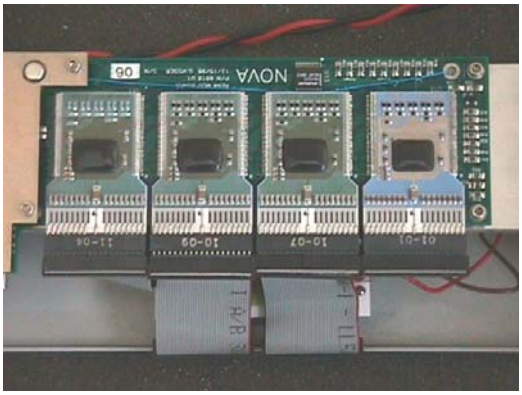

Figure 14. Photograph of 128-channel RENA ASIC system available at RMD for read-out of multi-element CZT/CdTe devices. Each chip has 32 channels & 4 chips are daisy chained. Shaping time is adjustable (0.4 to 6

4. ELECTRONIC READ-OUT ISSUES

For read-out of the proposed orthogonal strip and multi-pixel CdTe/CZT detectors, RMD had available several options. The orthogonal strip CdTe detector has 48 channels (40 high-resolution strips and 8 coarser DOI strips). The multi-pixel CdTe/CZT detectors require 37 channels, 36 anodes and one cathode.

One option for read-out of CdTe/CZT detectors was the 128 channel ASIC based electronics, RENA^{TM} – Read Out Electronics for Nuclear Applications, developed by NOVA R&D, Riverside, CA, that is available at RMD as shown in **Figure 14**. The RENA system has some interesting features such as global trigger, where all enabled channels are read when any channel is triggered (its signal level crosses the fixed threshold); sparse readout, where only the triggered channel(s) are readout; neighbor readout, where the triggered channel and its neighboring channels are readout; and select all, where all channels are readout when an external trigger is applied. RENA provides low noise operation for CdTe/CZT detectors. The shaping time in RENA can be adjusted in the 0.4-6 μs range. RENA chips (32 channels/chip) can be daisy chained up to 16 chips, which can all be readout as a single chip. RENA system has been setup at RMD in 128 channel format (using four chips) which was available for evaluation of CZT/CdTe detectors in the Phase I project. Many important performance characteristics of the CdTe/CZT detectors such as energy and spatial response can be evaluated using the RENA

system. However, the RENA system available at RMD is not suitable for fast timing, though its new version, RENA-II supports fast timing.

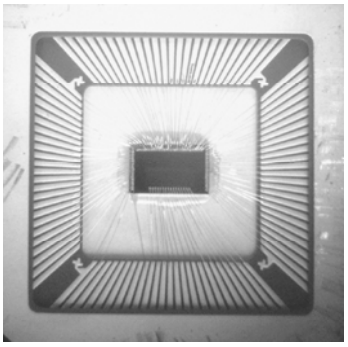

Figure 15a. A microscope photograph of RMD ASIC wire bonded to a 100-pin grid array. Note that the ASIC (central rectangle) is

As shown in **Figures 15a & 15b** as well as **Table 2**, RMD has recently built its own application specific integrated circuit (ASIC) for PET applications in collaboration with Augustine Engineering (Encinitas, CA). Each channel of the ASIC has a preamplifier, a shaper, and a peak hold stage that provides an analog output for energy information. In addition, a separate fast timing output is also provided. The specifications for RMD's ASIC are shown in **Table 2**. It should be noted that while this ASIC is originally designed for APD read-out, it is suitable for evaluation of the proposed CdTe/CZT detectors including fast timing studies (particularly for higher energy photons such as the 511 keV gamma-rays used in PET). CdTe/CZT detectors were successfully tested with RMD's ASIC in the Phase I project, which is very encouraging.

Table 2. RMD ASIC Specifications

Parameter	Specification
Channels	**16 channels**
Format	**Linear array**
Charge capacity	**$1x10^7$ e^-**
Risetime of preamp	**3-4 ns**
Conversion gain	**»1 V/pC, offset**
	115 e- rms slow, log

Finally, at RMD as well as UC-Davis, multiple sets of discrete preamplifiers, shapers and associated NIM electronics and data acquisition boards were available to allow evaluation of full-functionality of the proposed detectors (with limited number of orthogonal strips). The CdTe/CZT detectors were evaluated at RMD and at UC-Davis using ASIC as well as NIM electronics.

5. ELECTRICAL MEASUREMENTS OF CdTe/CZT DETECTORS

Once fabricated, CdTe/CZT detectors were tested, aimed mostly at revealing the critical electrical properties that dictate detector performance such as resistivity and charge transport parameters. These electrical measurements were made on simple, planar devices with metal-semiconductor-metal structure and ohmic electrodes. Devices with 10x10 mm^2 area and 4 mm thickness were used to measure these critical electrical parameters of CdTe and CZT crystals, prior to the evaluation of multi-pixel and strip detectors for PET imaging.

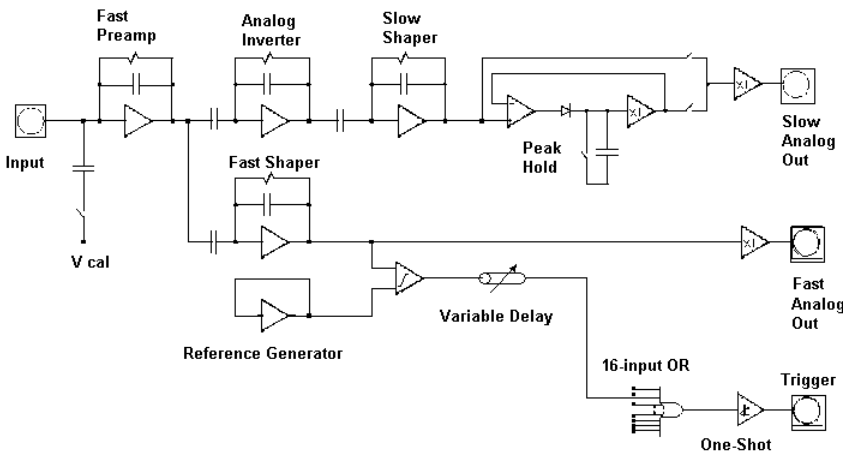

Figure 15b. Schematic diagram of one channel of a 16 channel linear ASIC built by RMD for fast timing applications such as PET.

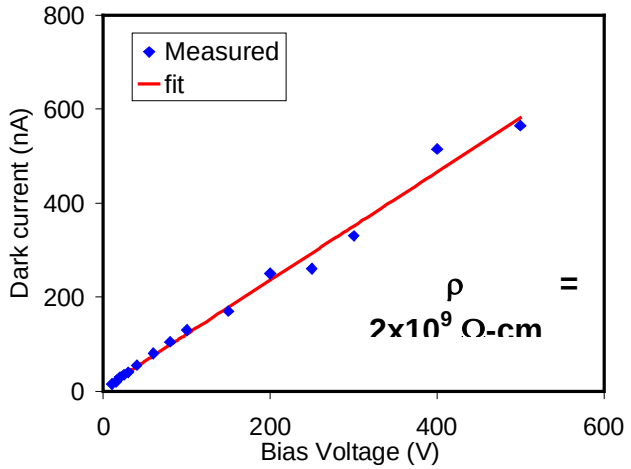

Figure 16. I-V curve for a CdTe crystal (10x10x4 mm^3). From this curve and the detector dimensions, the resistivity of the CdTe sample (from Accrorad) was estimated to be ~$2x10^9$ Ω-cm.

a. Resistivity

Low leakage current is an essential component of a photoconductive detector, particularly for distinguishing single photons or events. The steady state leakage current and the current induced by the charge carriers elevated to the conduction band upon excitation with a gamma-ray are superimposed and concurrently integrated on a capacitor (and subsequently discharged through several possible techniques, e.g. resistor, transistor reset). If the leakage current is too large, its RMS fluctuation produces 'pulses' (integrated charge) that acts as noise that degrades the spectral performance of the detector. Additionally, leakage current is generally dependent on applied bias. If an increased electric field is needed to prevent charge carriers from recombining too quickly and to provide fast response, then a larger leakage current must be expected. Constructing a detector from a material with high bulk resistivity is the most straightforward method of keeping the leakage current at acceptably low levels – generally considered to be a few hundred nA or less. From this limit and the expected device geometries (~10 mm^2 area/strip and 0.5 mm anode-to-cathode spacing, as shown in **Figure 1**), one should aim to maintain a bulk resistivity of 10^9 Ω·cm or greater. To best determine the bulk resistivity of the samples, current-voltage (I-V) data is taken. This is a simple and direct technique, and it immediately makes known any non-linearity. The experiments were setup to cover a range of several hundred volts. **Figure 16** shows I-V plots for a CdTe test device (10x10 mm^2 area, 4 mm thickness) built specifically for resistivity and charge transport measurements. From this data and the known device geometry, the resistivity of the CdTe bulk material (from Acrorad) was estimated to be ~$2x10^9$ Ω-cm at room temperature. Similar measurements were also carried out for a CZT detector (from Yinnel Tech.) and its resistivity was ≥10^{10} Ω-cm at room temperature.

b. Mobility-Lifetime Products

The figure of merit most commonly used to describe the ability of a semiconductor to transport charge within its bulk is the '$\mu\tau$' value or the mobility-lifetime product. Ionization creates a large number of electron-hole pairs within the active region of the detector. This only results in a large output signal if the charge carriers can have sufficient drift length, approaching the detector thickness, i.e., the distance between anode and cathode faces (or *d*). The most common technique for obtaining '$\mu\tau$' data is by observing the total amount of collected charge from an interaction (which is also referred to as charge collection efficiency, η/η_o) versus increasing applied detector bias (V_b). The data is collected as a pulse height spectrum with the detector under steady irradiation from, preferably, a monoenergetic source of shallowly penetrating radiation (such as 5.5 MeV α-particles, ^{241}Am source). The amount of collected charge is observed as the output signal of a charge sensitive preamplifier. A detector achieving

full charge collection is seen by spectral features (*e.g.* photopeak) reaching a maximum value that plateau without any further change upon bias increase. The data is fit to the single carrier Hecht equation [Hecht] and the μτ product of the charge carrier type being collected (electrons or holes, depending on the polarity of collecting electrode) is deduced as a parameter of the fit.

In our research, mobility-lifetime product (μτ) of electrons and holes in CdTe and CZT test detectors (10x10 mm^2 area and 4 mm thickness), built specifically for resistivity and charge transport studies, were measured by irradiating the respective contacts (negative contact for electrons, positive contact for holes) with alpha particles (~5.45 MeV alpha particles from an ^{241}Am source) and recording the location of the alpha peak as a function of voltage across the detector. The electronics for data collection consisted of a Cremat preamplifier (CR-110), Canberra 2020 spectroscopic amplifier and an Oxford PCA card installed in a computer. The range of the alpha particles in CZT/CdTe is ~20-30 μm which is significantly less than the thickness of the device. A single-carrier Hecht equation was then fit to the data using μτ as a fitting parameter.

$$\frac{\eta}{\eta_0} = \frac{(\mu\tau)V_b}{d^2}\left[1 - \exp\left(\frac{-d^2}{(\mu\tau)V}\right)\right]$$

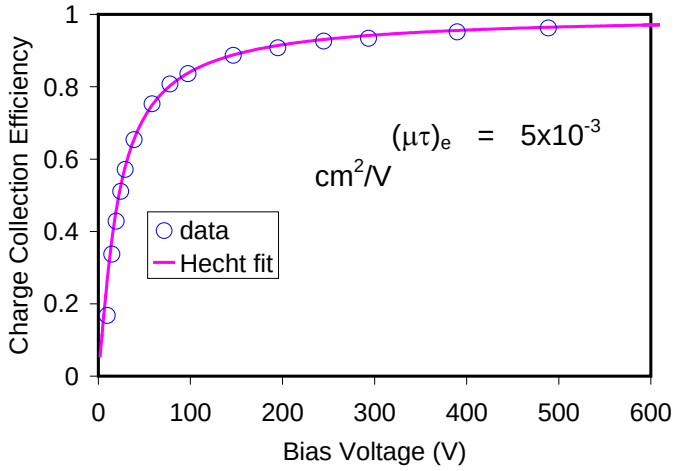

Figure 17. Charge collection efficiency (for electrons) versus bias for a CdTe crystal along with a fit to the data based on Hecht equation. From the fit, the mobility-lifetime product of electrons was estimated to be

Figure 17 shows a plot of charge collection efficiency (of electrons) versus applied voltage with the single-carrier Hecht equation fit to the measured data for a CdTe crystal (supplied by Acrorad, 10x10 mm^2 area and 4 mm thickness). The mobility-lifetime product of electrons for the CdTe sample is ~$5x10^{-3}$ cm^2/V. We have also performed a similar measurement (of mobility-lifetime product of electrons) for a CZT crystal from Yinnel. The mobility-lifetime product of electrons in this case is $7x10^{-3}$ cm^2/V. These results are encouraging and indicate that electron collection in both CdTe and CZT is very good.

Mobility-lifetime product of holes in CdTe and CZT was also measured and the results were $2x10^{-4}$ cm^2/V and $1x10^{-5}$ cm^2/V, respectively. Thus, hole collection is much superior in CdTe. In our detectors, particularly the orthogonal strip design, both electron and hole collection is essential for achieving high energy, timing and spatial resolution. As a result, CdTe was selected for fabrication of strip detectors in the Phase I effort. The resistivity and charge transport parameters (based on Phase I studies) and other detector parameters for CdTe and CZT are listed in **Table 3.**

Table 3. Measured Electrical and Transport Properties of CZT and CdTe

Material	Bandgap [eV]	Epair [eV]	Resistivity (ρ) [Ω-cm]	Mobility-Lifetime Product of Electrons $(\mu\tau)_e$ [cm^2/V]	Mobility-Lifetime Product of Holes $(\mu\tau)_h$ [cm^2/V]
CZT	~1.7	~5.0	$\geq 10^{10}$	$7x10^{-3}$	$1x10^{-5}$
CdTe	1.45	4.5	$2x10^{9}$	$5x10^{-3}$	$2x10^{-4}$

Note that E_{pair} in **Table 3** is the energy required to create an electron-hole pair. The E_{pair} values for CdTe and CZT are in 4.5 to 5 eV range, thus a 511 keV γ-ray interaction in these materials should produce ≥100,000 electron-hole pairs, which is ~10 times higher than the number of optical photons produced in a scintillator such as LSO for 511 keV interaction (~12,000 photons expected).

6. Energy & Timing Resolution Studies with Multi-Pixel Array

During the Phase I program, we have performed energy and timing resolution measurements with a multi-pixel CdTe array shown in **Figure 12**. The detector has 6x6 elements with 0.6 mm pixels and 1 mm thickness. The continuous cathode of the detector was irradiated with 511 keV gamma-rays (^{22}Na source) with a negative bias of 500 V applied to it and the signal from a selected anode pixel of the array was collected using a charge sensitive preamplifier (Tennelec #TC 170D and a spectroscopy amplifier (Canberra #2020). A ^{22}Na energy spectrum (511 keV gamma-rays) collected from one pixel of the multi-pixel array is shown in **Figure 18**. As seen in the figure, the energy resolution of the 511 keV gamma-ray peak is excellent, <2.5% (FWHM) at room temperature. This energy resolution is substantially better than that of a typical LSO-PMT detector which provides ~12-15% (FWHM) at 511 keV. ^{22}Na energy spectra were collected from all 36 pixels of the array shown in **Figure 12** and the average 511 keV energy resolution was <3% (FWHM).

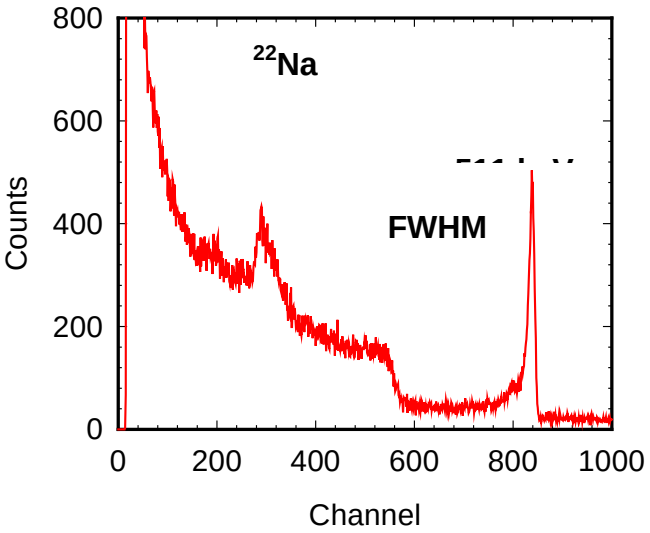

Figure 18. ^{22}Na spectrum collected with one pixel of CdTe array. The energy resolution of 511 keV photopeak is <2.5% (FWHM) at room temperature.

Timing resolution studies were also performed with the multi-pixel array operating in coincidence with a LSO-PMT reference detector. A schematic representation of the test setup is shown in **Figure 19**. The LSO-PMT detector formed the "start" channel in the timing circuit while the selected CdTe pixel formed the "stop" channel. Each detector was irradiated with 511 keV γ-ray pairs and the resulting coincidence timing

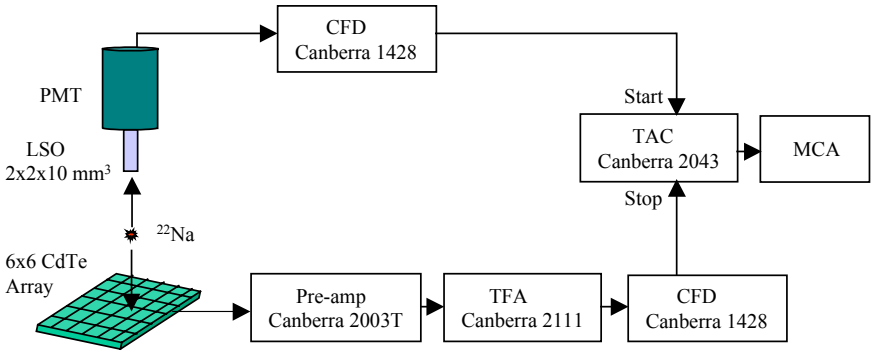

Figure 19. Schematic of the setup used to measure timing resolution of CdTe and CZT detectors in the Phase I effort.

spectrum is shown in **Figure 20**. The measured timing resolution was ~5.7 ns (FWHM). The timing resolution in this case is governed by the charge transport in the 1 mm thick array. Using a thinner semiconductor slab (0.5 mm), the timing resolution improved to ~4 ns (FWHM) at the same bias of 500 V.

Similar measurements were also performed using a 36 element CZT array (operated at 500 V) that had identical design to the CdTe array shown in **Figure 12** (0.6 mm pixels, 1 mm thickness). While the dark current in this case was lower (due to higher resistivity of CZT than CdTe), the energy and timing resolution were slightly worse due to poorer hole transport in the available CZT crystals. The energy resolution of a selected CZT pixel was ~4% (FWHM) at 511 keV. The timing resolution of a selected CZT pixel in coincidence with a LSO-PMT reference detector, measured using 511 keV gamma-ray pairs, was ~7.2 ns. Thus, the superior hole transport in CdTe is critical in enhancement of its overall performance for this particular application with our selected designs. CZT manufacturers (such as Yinnel, eV Products, Orbotech and others) continue to enhance the material properties (including hole transport) and as a result, we will continue to explore CZT along with CdTe in Phase II.

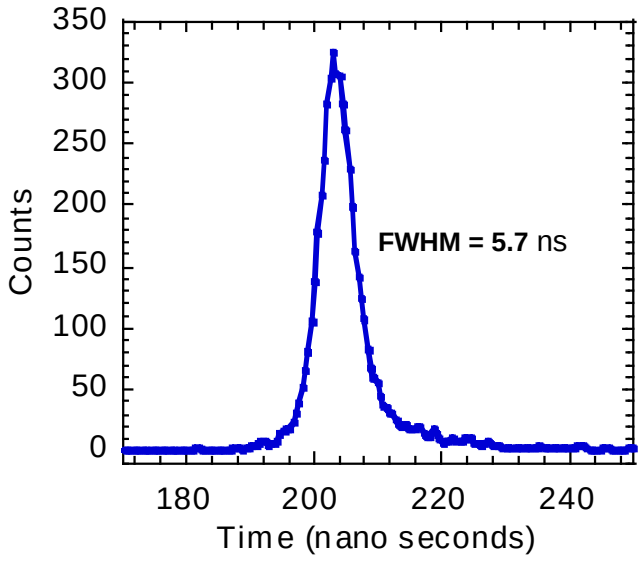

Figure 20. Timing spectrum acquired with multi-pixel CdTe array operating in coincidence with an LSO-PMT reference detector. The timing resolution is 5.7 ns (FWHM) at room temperature.

Overall, the results presented in this section are encouraging and indicate that multi-pixel CdTe arrays provide good performance. High resolution PET detectors for small animal imaging can be configured using multi-pixel arrays by stacking slabs of such multi-pixel arrays. High energy and timing resolution can be expected from each slab as demonstrated by the measurements in this section. Furthermore, due to fine-pixellation (~0.5 mm pixels), high spatial resolution can also be achieved. Finally, since separate read-out of each slab in the stack is required, very high DOI resolution is also expected. The main drawback of the stacking arrangement with multi-pixel arrays is the large number of read-out channels that would be required to achieve high detection efficiency, spatial resolution and imaging area. In order to overcome this issue, we have also evaluated an orthogonal strip detector design (see **Figures 1 & 2**), as discussed in the following section, which would significantly reduce the number of read-out channels.

7. Evaluation of CdTe PET Detector with Orthogonal Strip Design

The final aspect of the Phase I effort was to investigate the performance of the CdTe detector with orthogonal strip design. The orthogonal strip detector design was shown earlier in **Figure 1**, and photographs of fabricated and packaged CdTe strip detector were shown earlier in **Figure 2** and **Figure** 13, respectively. As discussed previously and illustrated in **Figures 1 & 2**, the detector was fabricated from a 20x20 mm^2 CdTe slab with 0.5 mm thickness. High resolution strips (0.5 mm pitch) were placed on one 20x20 mm^2 face and wider strips (2.5 mm pitch) were placed on the other face, perpendicular to the fine strips. Ultimately, in PET studies, the detector is designed for irradiation on the edge (0.5x20 mm^2 face, see **Figure 1**). The fine strips (0.5 mm pitch) along with the detector thickness of 0.5 mm provide an effective pixel size of 0.5 mm for incoming 511 keV γ-rays, with 20 mm depth available to stop these γ-rays. Furthermore, the wider strips with 2.5 mm pitch provide depth-of-interaction information. Such CdTe strip detectors were evaluated using discrete NIM electronics as well as ASIC electronics at RMD and UC-Davis in the Phase I effort.

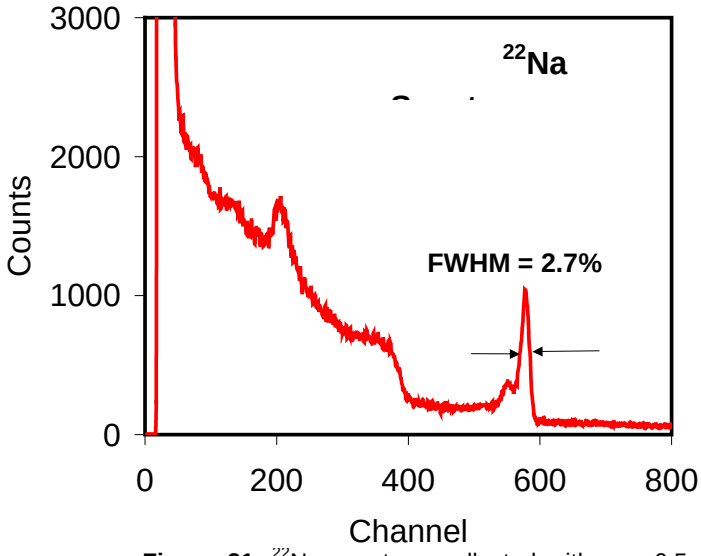

Figure 21. ^{22}Na spectrum collected with one 0.5 mm strip of the CdTe detector. The energy resolution of 511 keV photopeak is ~2.7% (FWHM) at room

Energy Resolution: As **Figure 21** shows, one of the first tasks was to check the energy response of fine strips (with 0.5 mm pitch) using 511 keV gamma-rays (^{22}Na source). This involved flood irradiation of the detector with all the wider cathode strips (2.5 mm pitch) biased to a negative potential of 100 V. Signal from each 0.5 mm strip was processed using a preamplifier and a shaping amplifier to generate an energy spectrum. **Figure 21** shows a ^{22}Na spectrum collected with one strip in this manner and the energy resolution of the 511 keV peak is ~2.7% (FWHM) at room temperature. The detector bias was varied from 100 to 500 V and the energy spectrum for the selected strip was measured as a function of detector bias. The energy resolution was found to be very similar across this range of detector bias. Similar spectra were collected for all 40 fine strips of the detector and the results are shown in **Figure 22**. Excellent energy resolution and uniformity were observed for all detector strips and the average 511 keV energy resolution was estimated to be <3.3% (FWHM), which is very encouraging.

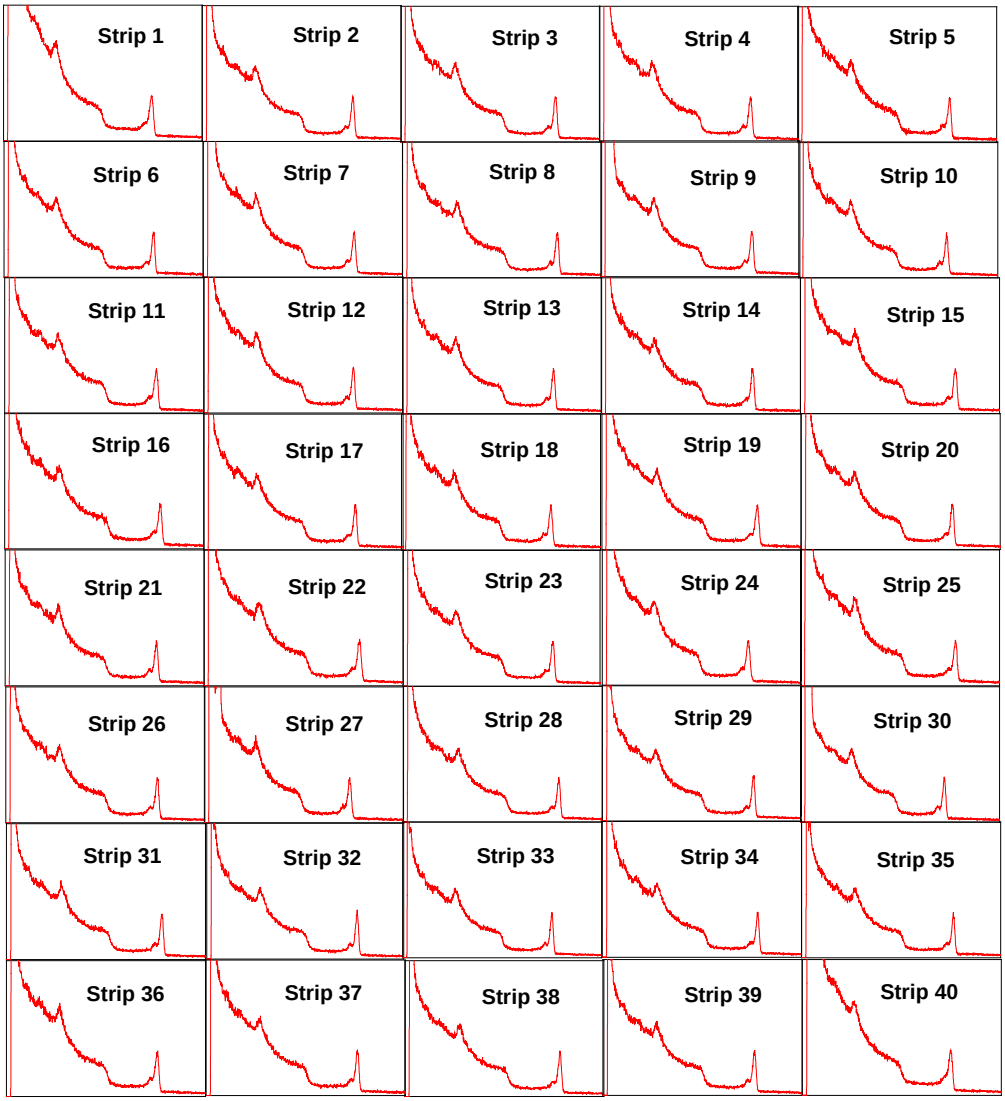

Figure 22. ^{22}Na spectra collected from all 0.5 mm strips of the orthogonal strip CdTe detector.

Timing Resolution: Timing resolution studies were also carried out using the orthogonal strip CdTe detector. All 2.5 mm cathode strips of the detector were biased to a negative potential of 500 V, while a selected 0.5 mm anode strip was used to generate the timing data. A schematic representation of the test setup used for the timing experiment was shown earlier in **Figure 19**. The CdTe strip detector was operated in coincidence with a LSO-PMT detector and the two detectors were irradiated with coincident 511 keV gamma-ray pairs. A coincidence timing spectrum generated for this configuration is shown in **Figure 23** and the timing resolution was estimated to be ~2.9 ns (FWHM) at room temperature. Timing studies were also carried out with the negative bias applied to cathode strips of the CdTe detector varied from 100 to 500 V, and as expected the timing resolution improved at higher detector bias (see **Figure 23**). This is primarily because the rise-time of the pulses for the CdTe detector becomes faster as the detector bias increases. As shown in **Figure 23** (right), at a detector bias of 200 V, the timing resolution is measured to be ~6.4 ns (FWHM) which is in good agreement with the simulation results

reported earlier. The timing response of several other strips was also measured and the results were found to be similar to those shown in **Figure 23**, which is very encouraging. These results confirm that the proposed CdTe strip detectors provide excellent energy and timing resolution.

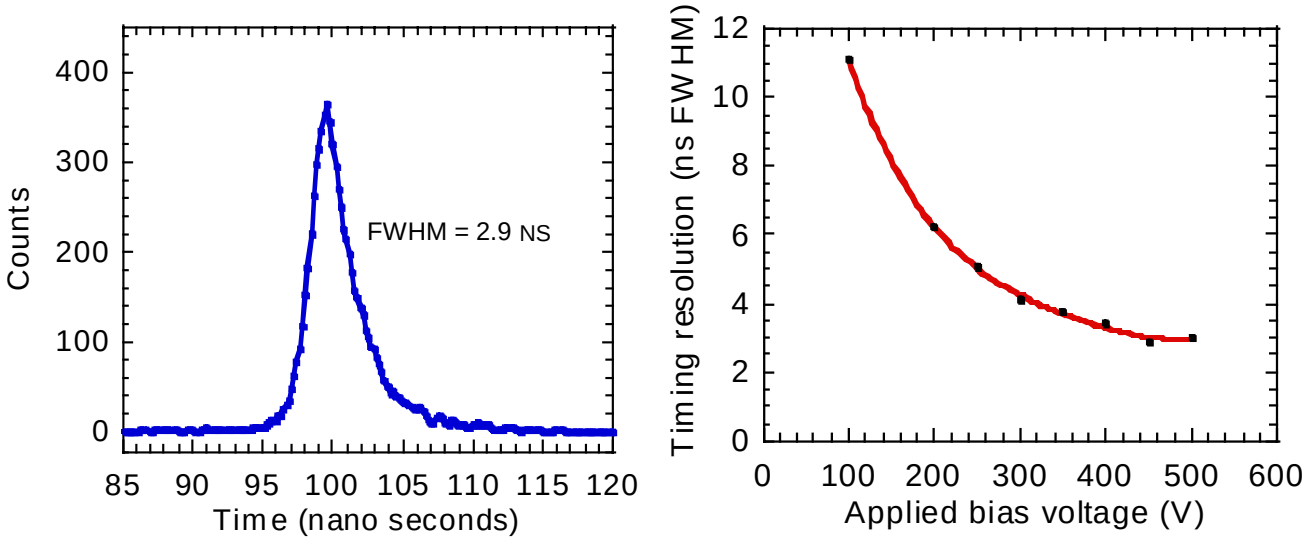

Figure 23. Timing resolution for a 0.5 mm strip of the CdTe detector (cathode strips biased at 500V, negative polarity) in coincidence with a LSO-PMT detector upon irradiation with 511 keV γ-ray pairs (left). On right, timing resolution for the same detectors is shown as a function of bias applied to cathode strips of the CdTe

Spatial Response of Finer Strips (0.5 mm pitch): The next series of experiments were aimed at investigating the spatial response of the detector, particularly using the fine strips with 0.5 mm pitch. In the first study (see **Figure 24a**), the detector was irradiated on the 20x20 mm^2 face with a collimated beam of 60 keV gamma-rays (^{241}Am source). In this study, 60 keV gamma-rays were chosen because they are relatively easy to collimate. Based on the Pb-collimator geometry and the collimator-to-detector distance, the diameter of the irradiated 60 keV spot on the detector face was estimated to be 0.4 mm. This spot was scanned (in 0.1 mm steps) across the 20x20 mm^2 detector face in orthogonal direction to the strips with 0.5 mm pitch as shown in **Figure 24a**.

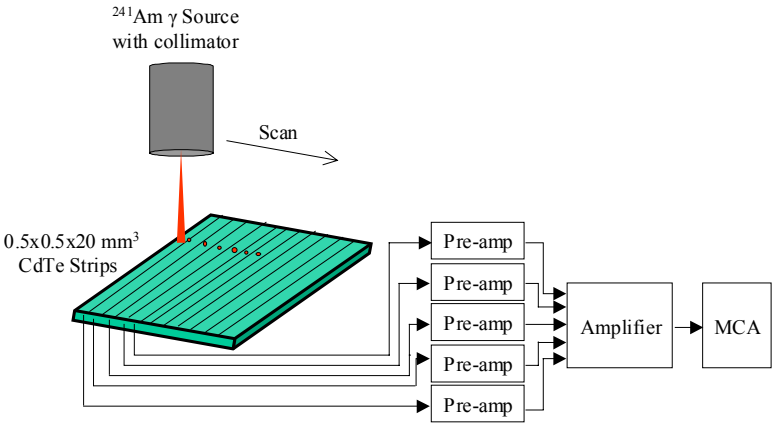

Figure 24a. Schematic of the experiment to measure spatial response of finer strips (0.5 mm pitch) using collimated 60 keV gamma-

For each source position, the count-rate response from five sequential strips (near the irradiated location) was measured. The result of this experiment during which the source was scanned across all five strips is shown in **Figure 24b**. The count-rate profile shown in **Figure 24b** demonstrates that each strip is well resolved, confirming that the detector displays excellent spatial resolution (essentially equivalent to the strip pitch). The average broadening of the peaks in the count-rate profile is ~0.5 mm (FWHM), as expected, which is very encouraging.

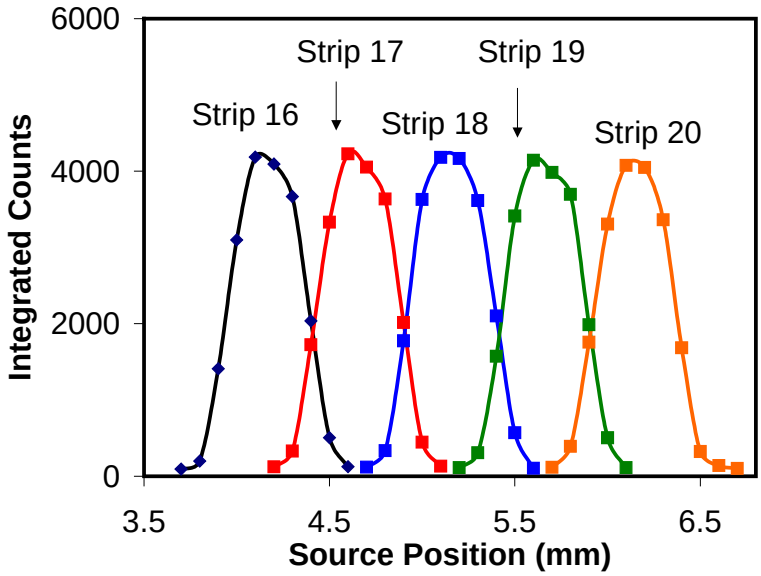

Figure 24b. Spatial response of a selection of five sequential strips (0.5 mm pitch) as a collimated beam of 60 keV gamma-rays is scanned across them in an orthogonal direction.

In addition to spatial response mapping demonstrated in **Figure 24b** with 60 keV photons, we have also measured the imaging response of the CdTe strip detector using higher energy gamma-rays in view of its intended use in PET application. While 511 keV gamma-rays are used in PET, we used gamma-rays with slightly higher energy (662 keV photons, ^{137}Cs source) in this study due to higher activity of the ^{137}Cs source available at RMD (compared to the available ^{22}Na source that emits 511 keV photons). This allowed completion of the experiment within a reasonable time-frame with gamma-rays having energy similar to that for the 511 keV positron annihilation photons. In this study, a collimated beam of 662 keV gamma-rays was incident on the detector edge (0.5x20 mm^2 face), which is the intended irradiation geometry for the detector. The 20 mm depth of CdTe provided reasonable stopping efficiency for the 662 keV gamma-rays. The collimated beam in this case was achieved with a slit in lead that was 0.25 mm wide, resulting in a 0.3 mm wide projection on the irradiated surface, which was scanned in

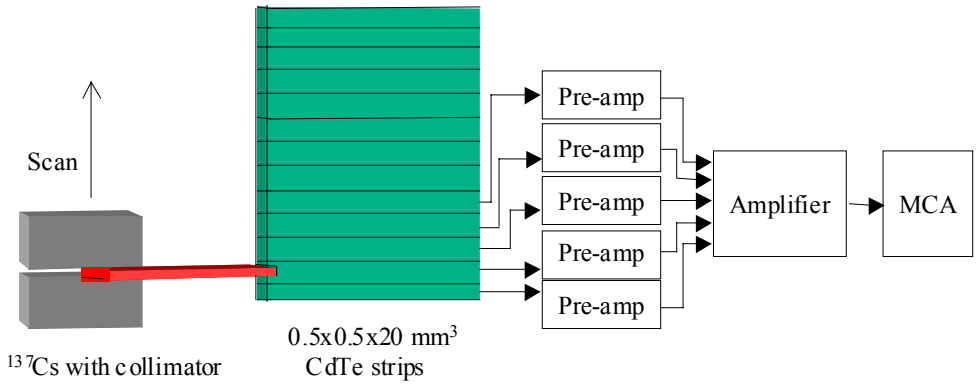

Figure 25a. Schematic of the experiment to measure spatial response of finer strips (0.5 mm pitch) using collimated 662 keV gamma-rays.

a direction orthogonal to the 0.5 mm strips (see **Figure 25a**). The resulting count-rate response of three sequential strips is shown in **Figure 25b**. Once again, each strip is well-resolved in the count-rate profile, confirming the high spatial resolution of the detector.

The response is slightly broader than that shown in **Figure 24b** primarily because the incident beam diverges more upon deeper penetration of γ-rays in the detector (which occurs due to high energy of the incident 662 keV gamma-rays with attenuation length of ~2 cm in CdTe). For example, a source projection of 0.3 mm on the irradiated face (x=0 mm) diverges to 0.5 mm at x = 20 mm. Inter-strip scatter also plays a role. Finally, a slight misalignment between the directions of the collimator slit and the high resolution strips would also cause more than one strip to be irradiated for each source position. Overall, the results in **Figure 25b** provide additional confirmation that the proposed detector design provides high spatial resolution (equivalent to the strip pitch) at gamma-ray energy very similar to that used in PET, which is very encouraging.

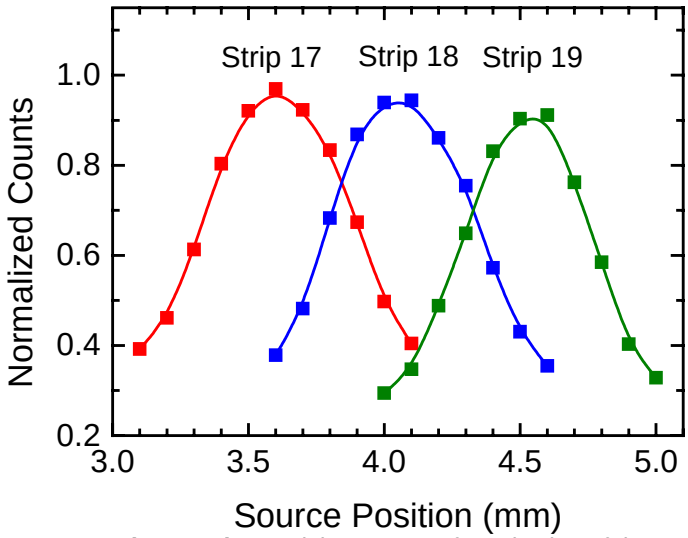

Figure 25b. Spatial response of a selection of three sequential strips (0.5 mm pitch) as a collimated beam of 662 keV gamma-rays is scanned across them in an orthogonal direction.

<u>Imaging Response of the Wider DOI Strips (2.5 mm pitch):</u> The next experiment was aimed at investigating the spatial response of the coarser strips with 2.5 mm pitch (see **Figure 26**) that are designed to provide depth-of-interaction (DOI) information (when the detector is irradiated from the edge as shown in **Figure 1**). To map the response of the coarser strips, we used similar experimental arrangement as that shown in **Figure 24a**, but in this case the source was scanned orthogonal to the coarser strips. Once again, 60 keV photons (^{241}Am source) were used because of high activity of the available ^{241}Am source and easier collimation of the 60 keV photons. The detector was irradiated on the 20x20 mm^2 face with a collimated beam of 60 keV gamma-rays (^{241}Am source). Based on Pb-collimator geometry and the collimator-to-detector distance, the diameter of the irradiated 60 keV spot on the detector face was estimated to be 0.4 mm. This spot was scanned across the 20x20 mm^2

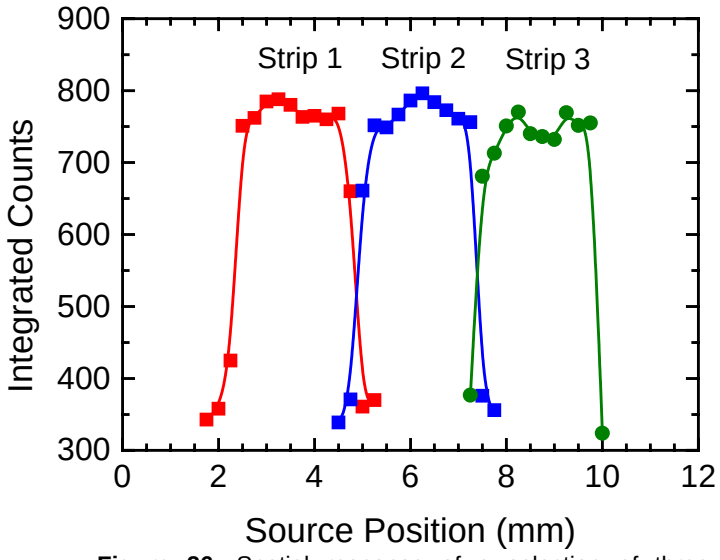

Figure 26. Spatial response of a selection of three sequential strips (2.5 mm pitch) as a collimated beam of 60 keV gamma-rays is scanned across them in an orthogonal direction.

detector face in orthogonal direction to the strips with 2.5 mm pitch. For each source position, the count-rate response from three sequential strips (near the irradiated location) was measured. The result of this experiment during which the source was scanned across all three selected strips is shown in **Figure 26**. The count-rate profile shown in **Figure 26** demonstrates that each strip is well resolved, confirming that the detector displays excellent DOI resolution (essentially equivalent to the pitch of the coarse strips). The average broadening of the peaks in the count-rate profile is ~2.5 mm (FWHM), which is very encouraging.

Intrinsic Position Resolution Studies: The final experiment in the Phase I project involved coincidence studies to determine the intrinsic position resolution of the CdTe strip detector using the finer strips with 0.5 mm pitch. This study was carried out at UC-Davis by Dr. Cherry's team.

In order to make an intrinsic position resolution measurement, the CdTe strip detector was fixed in its place, a small source placed some distance away, and on the other side of the source a PMT with small LSO pixels was positioned. The LSO pixels were 0.85x0.85 mm^2 and 15 mm long, and they were stacked to create a 0.85 mm wide, 10 mm tall, 15 mm thick detector facing the strip detector. **Figure 27** shows a schematic diagram of the setup where 511 keV gamma-ray pairs from a ^{18}F source irradiate both detectors.

Figure 27. Schematic diagram of the UC-Davis experimental setup used to measure the intrinsic position resolution of the CdTe strip detector (top view). The PMT with LSO crystals is shown on the left and moves back and forth as indicated by the arrows. The small ^{18}F source and the CdTe strip detector (high resolution strips with 0.5 mm pitch oriented vertically) are fixed.

As the PMT-LSO detector was moved back and forth, coincidence events between it and a selected, high resolution strip (0.5 mm pich) of the CdTe detector were recorded. Electronics for the setup included: for the PMT, a gain amplifier, a constant fraction discriminator which started two gates, and delay modules to set a coincidence window; and for the strip detector, a preamplifier, a spectroscopy amplifier set with 1 microsecond shaping time and a constant fraction discriminator. A counter/timer was used to count coincidences between the strip detector discriminator and the gate established by the PMT-LSO signal. For the source, a concentrated solution of ^{18}F was obtained and a small amount drawn into a 30 gauge needle (i.d. 150 microns, o.d. 310 microns). The 1-cm long needle was broken off, glued at the ends and then mounted on a fixture to create a source for the experimental setup shown in **Figure 27**. The long axis of the needle was parallel to the long axis of the strip of interest. As viewed from the strip detector, the LSO detector was 0.85 mm by 10 mm, with the long axis parallel to the needle and strip.

For this setup the distances were: LSO-to-strip detector distance of 75 mm, LSO-to-source distance of 60 mm, source-to-strip detector distance of 15 mm. The PMT-LSO detector was

moved back and forth and coincidences between LSO and the selected strip were recorded as a function of the LSO position. Normalizing the observed counts to the activity at the start of the measurement, and combining multiple measurements at each data point, a curve for relative counts versus position was obtained and is shown in **Figure 28.** For this figure, the position of the PMT was converted to effective position on the strip detector face using a multiplication factor of (15/60), and effects due to source size should be minimal in this arrangement. The result of the needle-source measurement is that the intrinsic position resolution of the CdTe strip is comparable to the 0.5-mm physical size of the strip-pitch as expected, which is very encouraging.

Overall, the results of the Phase I research confirm that proposed CdTe strip detector design provides excellent energy, timing, spatial, and DOI resolution and is therefore, very promising for small animal PET imaging. Thus, the feasibility of the proposed approach has been adequately demonstrated. Further advancement of the proposed detector design, including demonstration of a bench-top, prototype small animal PET scanner based on this novel detector design is planned for the Phase II effort.

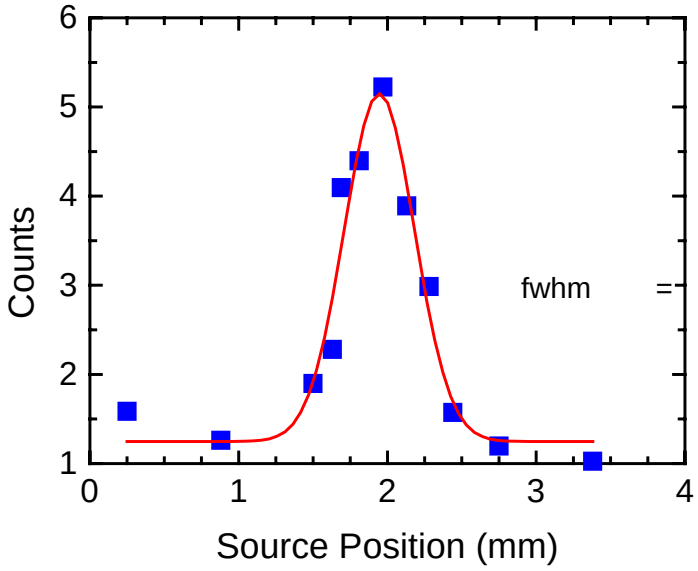

Figure 28. Coincidence event rate from a ^{18}F source versus effective position on the CdTe strip detector face. From the plot, the intrinsic spatial resolution of the